

# Anatomical Connectivity of the Subgenual Cingulate Region Targeted with Deep Brain Stimulation for Treatment-Resistant Depression

H. Johansen-Berg<sup>1</sup>, D. A. Gutman<sup>2</sup>, T. E. J. Behrens<sup>1,3</sup>, P. M. Matthews<sup>1,4,5</sup>, M. F. S. Rushworth<sup>1,3</sup>, E. Katz<sup>2</sup>, A. M. Lozano<sup>6</sup> and H. S. Mayberg<sup>2</sup>

<sup>1</sup>Centre for Functional MRI of the Brain, University of Oxford, Oxford OX3 9DU, UK, <sup>2</sup>Emory University School of Medicine, Atlanta, GA 30322, USA, <sup>3</sup>Department of Experimental Psychology, University of Oxford, Oxford OX1 3UD, UK, <sup>4</sup>Clinical Imaging Centre, Clinical Pharmacology and Discovery Medicine, GlaxoSmithKline, Hammersmith Hospital, London W12 0NN, UK, <sup>5</sup>Department of Clinical Neurosciences, Imperial College, London W6 8RF, UK and <sup>6</sup>Toronto Western Hospital, Division of Neurosurgery, Toronto, Ontario M5T 2S8, Canada

**Chronic deep brain stimulation (DBS) of subgenual cingulate white matter results in dramatic remission of symptoms in some previously treatment-resistant depression patients. The effects of stimulation may be mediated locally or via corticocortical or corticosubcortical connections. We use tractography to define the likely connectivity of cingulate regions stimulated in DBS-responsive patients using diffusion imaging data acquired in healthy control subjects. We defined 2 distinct regions within anterior cingulate cortex based on anatomical connectivity: a pregenual region strongly connected to medial prefrontal and anterior midcingulate cortex and a subgenual region with strongest connections to nucleus accumbens, amygdala, hypothalamus, and orbitofrontal cortex. The location of electrode contact points from 9 patients successfully treated with DBS lies within this subgenual region. The anatomical connectivity of the subgenual cingulate region targeted with DBS for depression supports the hypothesis that treatment efficacy is mediated via effects on a distributed network of frontal, limbic, and visceromotor brain regions. At present, targeting of DBS for depression is based on landmarks visible in conventional magnetic resonance imaging. Preoperatively acquired diffusion imaging for connectivity-based cortical mapping could improve neurosurgical targeting. We hypothesize that the subgenual region with greatest connectivity across the distributed network described here may prove most effective.**

**Keywords:** anterior cingulate, deep brain stimulation, depression, diffusion tractography, human, MRI

## Introduction

Chronic deep brain stimulation (DBS) of the white matter underlying the subgenual anterior cingulate cortex (sACC) results in dramatic remission of symptoms in some previously treatment-resistant patients (Mayberg et al. 2005). sACC is the part of the anterior cingulate cortex (ACC) located beneath the genu of the corpus callosum and corresponds primarily to Brodmann's area (BA) 25, as well as the caudal portions of BA32 and BA24. It is functionally and cytoarchitecturally distinct from the more dorsal part of the anterior cingulate, located anterior to the genu, comprising BA32 and inferior parts of BA24 (Carmichael and Price 1994; Vogt et al. 1995, 2005). It has been postulated that sACC may be a critical hub within distributed networks mediating depressive symptoms (Mayberg 2003; Seminowicz et al. 2004). Previous brain imaging studies have implicated sACC in experience of negative mood states (George et al. 1995; Mayberg et al. 1999). The volume of

sACC is reduced in certain depressed groups (Botteron et al. 2002; Coryell et al. 2005). Decreases in sACC activity have been reported following successful treatment of depression with a variety of nonsurgical interventions including pharmacological treatments (Mayberg et al. 2000; Drevets et al. 2002), electroconvulsive therapy (Nobler et al. 2001), and transcranial magnetic stimulation (Mottaghy et al. 2002).

The subgenual cingulate region does not act in isolation but rather forms part of distributed corticolimbic circuits that are putatively disrupted in patients with mood disorders. Overactivation of limbic regions including the hypothalamus and amygdala and underactivation of medial prefrontal cortex have been observed during performance of a sustained attention task in patients with bipolar disorder studied when euthymic (Strakowski et al. 2004). Resting blood flow recordings reveal hypoperfusion across a network of frontoparietal regions and hyperperfusion in subgenual cingulate and anterior insular cortices both in mood disorder and also with induction of transient sadness in healthy subjects (Mayberg et al. 1999; Liotti et al. 2002). Successful treatment of mood disorder results in a relative normalization of these activity patterns (Mayberg et al. 1999, 2005; Goldapple et al. 2004; Kennedy et al. 2007). Failure to respond to treatment can be predicted by altered functional interactions across a corticolimbic circuit including sACC (Seminowicz et al. 2004). These findings are consistent with the view that depression does not result from localized disruption to specific brain regions but rather as a consequence of dysfunction in distributed limbic-cortical brain systems (Mayberg 1997; Nestler et al. 2002).

Therapeutic effects of DBS may therefore be mediated via anatomical connections between the stimulated region and distributed cortical and subcortical areas. Tracer studies in nonhuman primates have shown that sACC has reciprocal cortical connections with orbitofrontal, dorsomedial prefrontal, dorsolateral prefrontal, and dorsal cingulate cortices (Vogt and Pandya 1987; Carmichael and Price 1996). Dense subcortical connections with the hypothalamus (Ongur et al. 1998; Freedman et al. 2000; Barbas et al. 2003), ventral striatum (Kunishio and Haber 1994; Haber et al. 1995, 2006; Ferry et al. 2000), amygdala (Freedman et al. 2000), and autonomic centers in the brainstem including the periaqueductal gray (An et al. 1998; Freedman et al. 2000) are consistent with a postulated role of sACC in visceromotor control. However, the connections of sACC specifically have not previously been studied in the human brain, and the pathways running through the white matter region underlying sACC and targeted in DBS have not been established.

Currently, surgical targeting of the sACC region has been based on the location of previously reported cross-group changes in blood flow and metabolic positron emission tomography (PET) signals (Mayberg et al. 2005). However, given the localized regional variations in cytoarchitecture, chemoarchitecture, and anatomical connectivity that have been reported in nonhuman primates (Carmichael and Price 1994, 1996; Vogt et al. 2005), it is possible that slight variations in electrode placements could have a substantial impact on outcome. Only preliminary data concerning the anatomical connectivity of ACC are available for the human brain (Croxson et al. 2005), and regional variations in connectivity between subregions of human ACC have not previously been investigated. Therefore, characterization of the variability of perigenual ACC connectivity in healthy controls is a first step to evaluating patient variability and ultimately individualized targeting of the white matter bundle based on likely connectivity patterns. Such studies may further inform on mechanisms mediating response or nonresponse to seemingly comparable electrode placement in treatment-resistant patients. Here, we characterize the anatomical connectivity of the perigenual ACC region in healthy control subjects. First, we test for connections between the perigenual ACC region and remote areas shown in a previous study to display altered functional responses following DBS (Mayberg et al. 2005) to test whether anatomical pathways underlie these altered functional responses. Next, we perform a connectivity-based parcellation of the ACC region, allowing us to contrast connection patterns of the perigenual ACC and sACC with all other voxels in the brain. This parcellation approach does not depend on definition of regions of interest (ROIs) and considers all traceable connections of the ACC. Finally, we project the precise sites of DBS electrodes from 9 successfully implanted patients onto the resulting connectivity-based parcellation of perigenual ACC to define the anatomical pathways likely to be affected by stimulation.

We use diffusion-weighted magnetic resonance imaging (DWI) to gain information on anatomical connectivity non-invasively. In brain white matter, self-diffusion of water molecules is directionally dependent and the principal diffusion direction corresponds to the predominant direction in oriented fiber bundles (Beaulieu and Allen 1994). By modeling local diffusion properties, it is possible to estimate these directions and to follow them using probabilistic tractography (Behrens, Johansen-Berg, et al. 2003). We have previously used this approach to characterize the connectivity of subcortical (Behrens, Johansen-Berg, et al. 2003; Johansen-Berg et al. 2005) and brainstem (Sillery et al. 2005; Hadjipavlou et al. 2006) structures, as well as cortical areas (Johansen-Berg et al. 2004; Rushworth et al. 2006), including prefrontal cortex and ACC (Croxson et al. 2005). Pathways traced in this way are reproducible (Heiervang et al. 2006) and generally reproduce those identified using postmortem dissection or tract tracing (Stieltjes et al. 2001; Croxson et al. 2005). In addition, information from tractography can be used to parcellate gray matter structures based on their anatomical connectivity (Johansen-Berg et al. 2004; Anwander et al. 2007), allowing for functionally relevant, reproducible, microstructural borders to be defined noninvasively in the human brain (Behrens and Johansen-Berg 2005; Klein et al. 2007). Recent advances in modeling of local diffusion properties allow estimation of more than 1 fiber direction at each voxel, enabling tracing of crossing

fibers (Behrens et al. 2007), a particular benefit when studying cingulate anatomy, as pathways to and from the cingulate cortex tend to be difficult to trace given the proximity of the corpus callosum and cingulum bundle.

## Methods

### *Diffusion Magnetic Resonance Data in Healthy Controls*

We acquired diffusion-weighted images ( $72 \times 2$ -mm-thick axial slices, matrix  $128 \times 104$ , field of view  $256 \times 208$  mm, giving a voxel size of  $2 \times 2 \times 2$  mm) in 17 healthy subjects (11 males, 6 females, aged 20–38 years) using a 1.5-T Siemens Sonata scanner with maximum gradient strength of  $40 \text{ mTm}^{-1}$ . The diffusion weighting was isotropically distributed along 60 directions using a  $b$  value of  $1000 \text{ smm}^{-2}$ . A  $T_1$ -weighted anatomical image was acquired for each subject using a 3D FLASH sequence (repetition time = 12 ms, echo time = 5.65 ms, and flip angle =  $19^\circ$ , with elliptical sampling of  $k$  space, giving a voxel size of  $1 \times 1 \times 1$  mm in 5 min and 5 s). All subjects were right handed, with no history of psychiatric or neurological disease. Informed written consent was obtained from all subjects in accordance with ethical approval from the Central Office for Research Ethics Committees, UK.

### *Diffusion Image Analysis*

Diffusion images were processed using FMRIB's Diffusion Toolbox (Behrens, Woolrich, et al. 2003; Smith et al. 2004) ([www.fmrib.ox.ac.uk/fsl](http://www.fmrib.ox.ac.uk/fsl)). We skull stripped (Smith 2002) diffusion-weighted,  $T_1$ -weighted, and Montreal Neurological Institute standard brain template images (Evans et al. 2003) and performed affine registration (Jenkinson and Smith 2001) to derive transformation matrices among the 3 spaces. We fitted a multi-fiber diffusion model (Behrens et al. 2007) that estimates probability distributions on the direction of 1 or more fiber populations at each brain voxel. Probabilistic tractography was then performed from any brain voxel by tracing streamline samples through these probabilistic distributions on fiber direction. For all tractography, we generated 25 000 streamline samples from each seed voxel to build up a connectivity distribution. The number of these samples passing through each brain voxel is interpreted as proportional to the probability of connection to the seed voxel. By fitting a multi-fiber model to our diffusion data, we were able to trace pathways through regions of fiber crossing (Behrens et al. 2007).

### *Distribution of Connections from Perigenual Cingulate to Areas of Functional Change Following DBS*

A previous PET study identified a network of regions that showed altered regional cerebral blood flow responses following chronic subgenual DBS (Mayberg et al. 2005). Little is known about the anatomical connections of these regions in the human brain, and we wished to test whether anatomical pathways from the ACC could underlie these altered functional responses. We therefore defined target ROIs based on the regions showing altered PET responses and characterized the connectivity of the whole perigenual cingulate region to these target ROIs. We defined a seed ROI as a large ventral perigenual ACC mask and defined target ROIs in several brain regions identified by Mayberg et al. (2005) including the amygdala (AMYG), anterior midcingulate cortex (AMCC), frontal pole (FP), hypothalamus (HTH), nucleus accumbens (NAC), orbitofrontal cortex (OFC), and dorsal medial frontal cortex (DMF) (Fig. 1). We generated probabilistic connectivity distributions from all voxels within the ventral ACC ROI and quantified their probability of connection to each target ROI. Voxels within the perigenual ACC ROI were classified according to their probability of connection with each of the target regions as in previous studies (Behrens, Johansen-Berg, et al. 2003; Johansen-Berg et al. 2005; Ramnani et al. 2005). Note that these target ROIs are defined according to functional criteria (PET activation changes following DBS) rather than anatomical criteria. These areas of PET activation change following DBS will not include all areas that are anatomically connected with the perigenual ACC region. This initial analysis is therefore limited to defining the distribution of

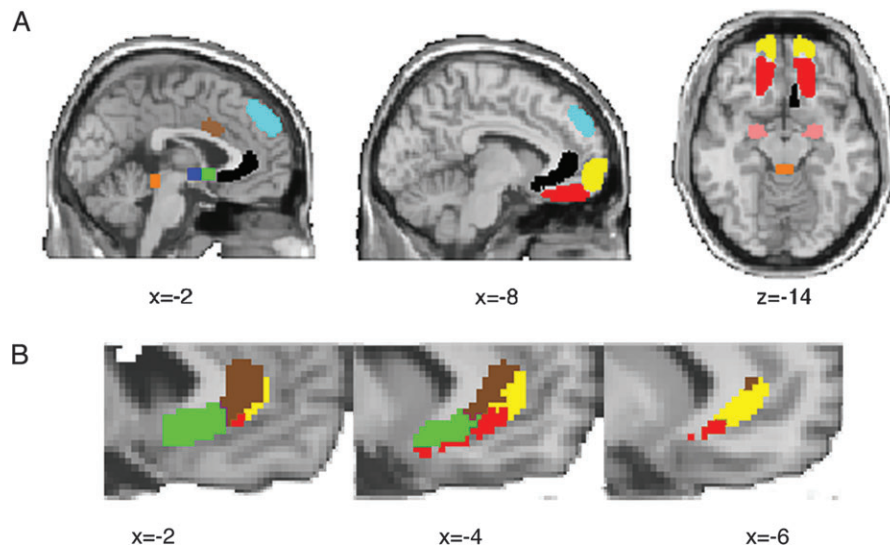


**Figure 1.** Distribution of connections involving ACC. (A) Locations of target ROIs defined based on change in regional cerebral blood flow in a previous PET study of chronic subgenual DBS. Pink = amygdala (AMYG); brown = anterior mid cingulate (AMCC); blue = hypothalamus (HTH); green = nucleus accumbens (NAC); light blue = dorsal medial frontal (DMF); red = orbitofrontal (OFC); yellow = frontal pole (FP); orange = periaqueductal gray (PAG); also shown in black is the perigenual seed mask. (B) Dominant connections from ACC to areas showing significant functional changes following DBS. ACC voxels from within the seed ROI are color coded according to the target region with highest probability of connection only. Colors match those used for ROIs in (A): brown = AMCC; yellow = FP; green = NAC; red = OFC. Note that this representation shows only the most probable connection for each ACC seed voxel. Many voxels show connections to more than 1 target ROI (see Fig. 2).

connections between perigenual ACC and areas of significant PET activity change following DBS. Subsequent analyses do not depend on definition of these initial ROIs and may therefore provide a more complete picture of the connectivity of the perigenual ACC.

#### Blind Parcellation of Perigenual Cingulate

We used “blind” connectivity-based parcellation (Johansen-Berg et al. 2004) to detect whether there are regions of distinct connectivity within the perigenual ACC ROI. This process is fully described elsewhere (Johansen-Berg et al. 2004; Klein et al. 2007). Briefly, probabilistic tractography was run from each voxel within the perigenual ACC ROI. The probability of connection from each seed voxel (at  $2 \times 2 \times 2 \text{ mm}^3$  resolution) to every other voxel in the brain (stored at low-resolution,  $5 \times 5 \times 5 \text{ mm}^3$ , for computational reasons) was binarized and stored in a matrix,  $A$ , of dimensions (number of seed voxels [high-resolution]  $\times$  number of voxels in the rest of the brain [low-resolution]). The cross correlation matrix of  $A$  was computed, resulting in a symmetrical matrix,  $B$ , of dimensions (number of seeds  $\times$  number of seeds [high-resolution]) in which the  $(i,j)$ th element value is the correlation between the connectivity profile of seed  $i$  and seed  $j$ . The nodes in  $B$  were permuted using a spectral reordering algorithm (Barnard et al. 1995) that finds the reordering that minimizes the sum of element values multiplied by the squared distance of that element from the diagonal, hence forcing large values toward the diagonal. If the data contain clusters (representing seed values with similar connectivity), then these clusters will be apparent in the reordered matrix, and break points between clusters will represent locations where connectivity patterns change. Clusters were identified by eye as groups of elements that were strongly correlated with each other and weakly correlated with the rest of the matrix. Elements that did not clearly belong to a single cluster were left unclassified.

Population probability maps of resulting clusters were derived by overlapping these clusters (in standard brain space) across subjects and dividing by the number of subjects so that voxel values in the population probability maps represent the proportion of the population in whom a cluster is present. Population probability maps were then thresholded to include only those voxels present in at least 50% of the

population and using a color scale ranging from red (50%) to yellow (>80%).

#### Projecting Electrode Sites in Patients onto Connectivity-Based ACC Parcellation

We used routinely acquired postoperative magnetic resonance scans to locate electrodes in 9 patients treated with subgenual cingulate white matter DBS for treatment-resistant depression. Inclusion and exclusion criteria, informed consent process, and surgical procedures have been described elsewhere (Mayberg et al. 2005). Briefly, DBS quadripolar electrodes (Medtronic 3387; Medtronic Inc, Minneapolis, MN) were implanted bilaterally in the ventral ACC white matter. Prior to surgery, the target was identified on a midline  $T_1$  sagittal image; during surgery, the target was located with reference to a stereotactic frame fixed to the patient's head. Each of the 4 electrode contacts was tested for adverse effects and clinical benefits. Clinical outcome after 6 months of chronic stimulation was evaluated using previously described scales, and only patients who showed a sustained response to chronic stimulation were considered (Mayberg et al. 2005).

Coverage, contrast, and image quality were variable for postoperative magnetic resonance imaging (MRI) scans, and so automated registration to a standard brain template was not consistently accurate for the perigenual cingulate ROI. Locations of electrode contacts used for stimulation were therefore projected manually onto a standard brain based on distances from clearly visible local landmarks (e.g., edges of ventricles, corpus callosum) by an experimenter blind to the connectivity-based parcellation.

## Results

#### Distribution of Connections from the Perigenual ACC to Areas of Functional Change Following DBS

We seeded all voxels within the perigenual ACC ROI (black mask in Fig. 1A) and quantified the probability of connection to several remote, predefined cortical and subcortical target masks (colored masks in Fig. 1A) that had previously been



shown to have altered functional responses following chronic subgenual DBS. We found evidence for anatomical pathways between ACC and these remote areas. The distribution of connections, within the perigenual ACC, to each of these other brain regions is seen in Figure 2. Although connections to many of the target ROIs are present throughout the perigenual ACC, the strength of these connections varies depending on the location within the ACC. Connections with the amygdala, hypothalamus, NAC, and OFC are strongest in the more posterior, subgenual part of the ACC (Fig. 2). Connections with the AMCC and FP are more prominent in the pregenual cingulate (Fig. 2).

Figure 2 demonstrates that, within the perigenual ACC, there is significant overlap in the distribution of connections with the different functionally defined target areas in the rest of the

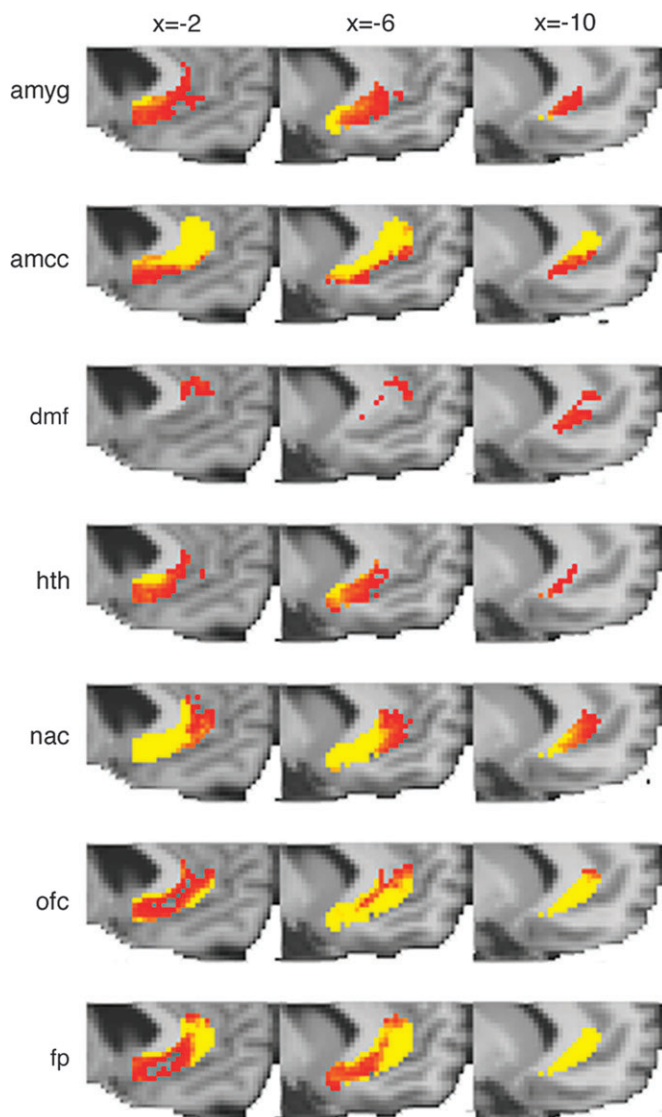


**Figure 2.** Distribution of connections from the perigenual cingulate seed ROI to target ROIs showing significant functional changes following DBS. Group average results showing voxels within the ACC seed ROI, which connected to each target ROI. The color scale indicates probability of connection from low (red, >50/5000 paths from seed voxel reach target ROI) to high (yellow, >500/5000 paths from seed voxel reach target ROI) (no voxels connecting to periaqueductal gray were found). Abbreviations for each target mask are defined in Figure 1.

brain. However, there are also regions that are dominated by connections to particular targets. To segment the perigenual ACC region on the basis of the most dominant connections, we classified each voxel according to the target region with which it had the highest probability of connection (Fig. 1B, color coding refers to target ROIs in Fig. 1A). The dominant connections were with AMCC from the most dorsal parts of the perigenual ACC seed ROI, with FP in the most anterior-lateral parts of the seed ROI, and with OFC in the inferior parts of the seed ROI (Fig. 1B).

Note that this analysis depends on our initial selection of target ROIs, chosen as sites of activation change in a previous PET study of DBS. There will be additional regions, not included in this ROI-based analysis, that are anatomically connected with the perigenual ACC. Our subsequent analyses did not depend on predefinition of any target ROIs and should therefore identify additional connections of interest.

### Connectivity-Based Parcellation of the Perigenual ACC

Automated, “blind” connectivity-based parcellation defined 2 regions with distinct connectivity within the ventral ACC region for each individual. These were combined in standard brain space to create a probabilistic, population-based parcellation of the perigenual ACC ROI into 2 subregions: a pregenual ACC (pACC, red to yellow, Fig. 3A,B) and an sACC (dark blue to light blue, Fig. 3A,B). To determine the major differences in connection patterns that had driven this connectivity-based parcellation, we used the sACC and pACC regions as seeds for probabilistic tractography (Fig. 4). Figure 4(A–F) shows pathways from pACC (red to yellow) or sACC (blue to light blue). Figure 4(G–I) again illustrates paths from pACC in red and sACC in blue but also highlights pathways that are common to pACC and sACC in green. Although there are some common areas of strong connectivity for both sACC and pACC (e.g., midcingulate, FP, hypothalamus, and NAC), we also defined clear differences in connection strength for particular pathways. Differences in connection patterns between the 2 regions are what drive the connectivity-based parcellation. There are apparent differences in the strength of connections from pACC and sACC to particular brain regions that may be of interest. For example, the pACC is more strongly connected to the FP and does not connect as strongly with medial temporal lobe (Fig. 4A,B,G,H). By contrast, the sACC region is more strongly connected to OFC, fornix, and the medial temporal

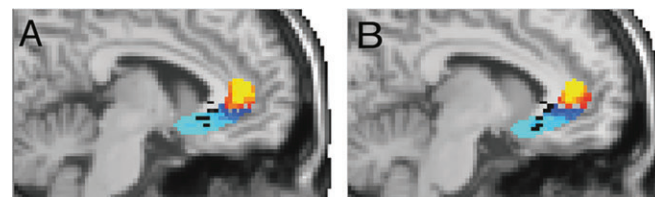


**Figure 3.** Connectivity-based parcellation of ACC and location of electrode contacts. (A, B) Population probability maps of connectivity-defined sACC and pACC. Color scales represent the population probability of a voxel belonging to sACC (from 50% [dark blue] to 80% [light blue] probability) or pACC (from 50% [red] to 80% [yellow] probability). Also shown are the locations of effective electrode contacts from 9 patients overlaid in black. Effective electrode locations are mainly localized within the sACC subregion. A is located at X = −6 and B at X = −8.

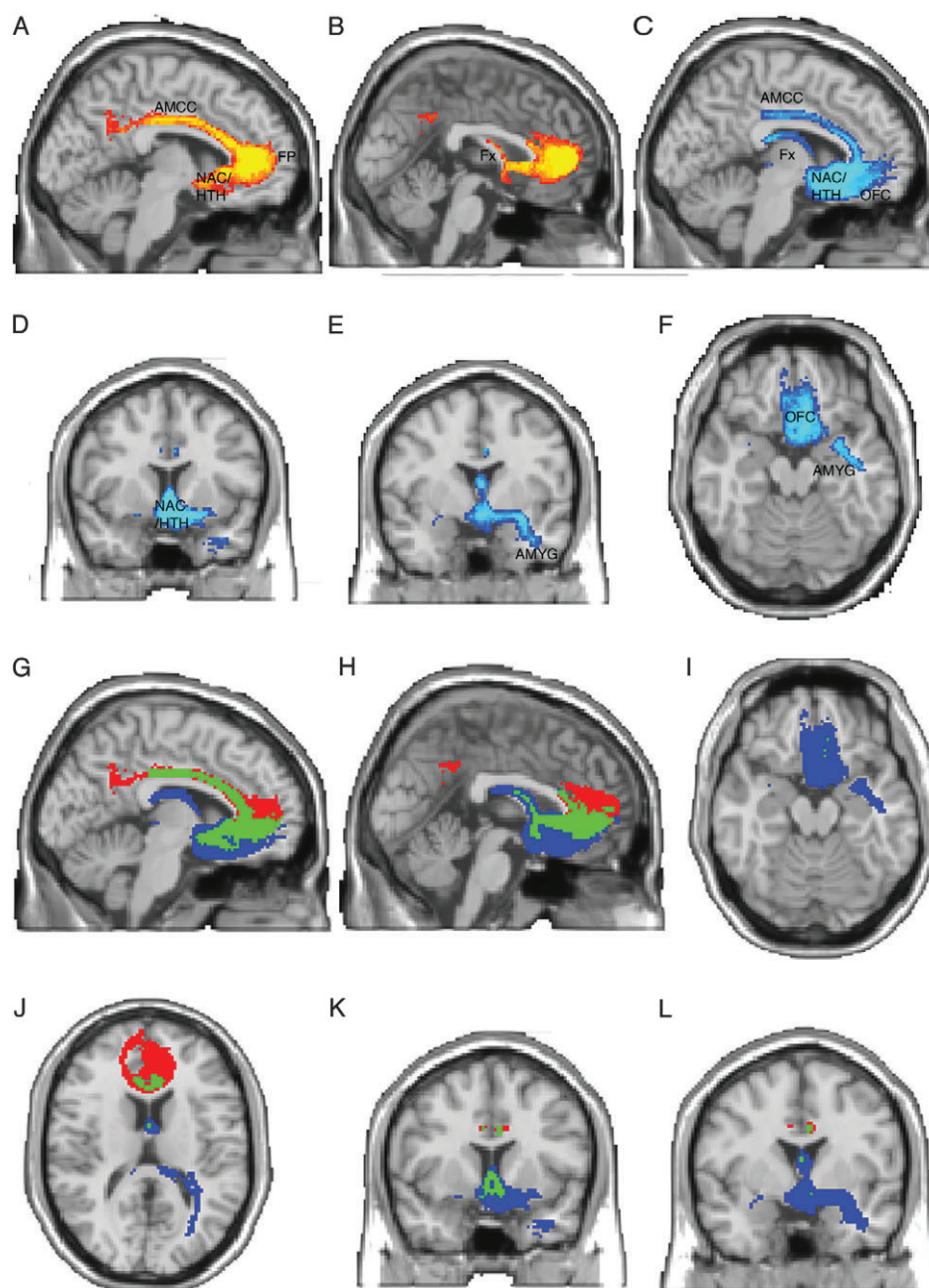


**Figure 4.** Tracts from sACC and pACC regions. (A–F) Population maps of results of probabilistic tractography from the pACC and sACC subregions. Color scales represent the population probability of a voxel belonging to a pathway from pACC (A, B, red to yellow) or sACC (C–F, dark blue to light blue). Abbreviated labels indicate gray matter regions that are connected with sACC or pACC via these pathways. (Note that the labels identify the pathways, rather than the gray matter structures themselves, which may not be visible in all views). (A, B) Pathways from pACC connect with the AMCC (A), FP (A), NAC (A), hypothalamus (A), and fornix (B). Color scale represents population probability of a pathway being present from 50% (red) to 80% (yellow). (C, D, E, F) Pathways from the sACC connect with the OFC (C, F), NAC (C, D), hypothalamus (C, D), AMCC (C), fornix (C), and amygdala (E, F). Color scale represents population probability of a pathway being present from 50% (dark blue) to 80% (light blue). Panels G–L overlay paths from pACC (red) and sACC (blue) and indicate areas of overlapping paths (green). Note that these representations depend somewhat on the degree of thresholding applied to the pathways. Here, we show paths present in at least 50% of subjects. Using a lower threshold would give greater overlap between sACC and pACC paths, whereas a higher threshold would give less overlap.

lobe in the vicinity of the AMYG and anterior hippocampus (Fig. 4C–L).

#### Projection of Electrode Locations onto Connectivity-Based Parcellation

We projected active electrode contact points from patients' postoperative MRI scans onto the population parcellations of

the perigenual ACC ROI (Fig. 3A,B). When the sACC population probability map was thresholded to include voxels classified as sACC in >50% of the population (as in Fig. 3), the majority (6/9) of effective stimulated electrode points were located within this sACC region (Fig. 3A,B). The remaining 3/9 were located just outside the superior border of the 50% thresholded sACC region (visible toward callosal white matter in Fig. 3A,B).



None were located within the pACC white matter population map.

## Discussion

Diffusion tractography revealed that the subgenual and pregenual portions of the human anterior cingulate (sACC and pACC) have distinct patterns of connectivity. The effective action of DBS for depression, which mainly targets the subgenual portion, may be mediated via strong connections to OFC, AMCC, hypothalamus, NAC, and amygdala/hippocampus.

Elucidation of these anatomical connections in the human brain should help to inform future studies of the functional interactions both in the healthy brain and in depressed subjects. Decreased functional connectivity between perigenual cingulate and amygdala has previously been observed in subjects with the short allele polymorphism of the serotonin transporter gene (Pezawas et al. 2005). Here, we were able to trace anatomical connections between sACC and amygdala, a path that has proved difficult to trace with previous methods (Behrens et al. 2007), providing an approach that could be used to test for a relationship between the anatomical strength of this pathway and depression susceptibility or treatment responsiveness. Such a relationship might be predicted based on previous studies that have found an association between treatment response and measures of functional connectivity between interconnected nodes within sACC circuits (Seminowicz et al. 2004).

A previous PET study demonstrated altered regional cerebral blood flow in a number of cortical and subcortical regions following chronic subgenual DBS for depression (Mayberg et al. 2005). We found evidence for anatomical pathways linking the perigenual ACC with these remote areas, providing a potential anatomical substrate for these altered functional responses. Connections with regions of altered functional response in the amygdala, NAC, hypothalamus, and OFC were stronger from the subgenual part of our perigenual ACC ROI.

We previously used DWI tractography to characterize the connectivity of the human and macaque frontal cortex (Croxson et al. 2005). In that study, we considered connections of the whole cingulate gyrus, without separating out different subregions. Consistent with our current findings on the connectivity of sACC specifically, we previously found prominent connections between cingulate gyrus and amygdala, cingulum bundle, and NAC in both human and macaque (Croxson et al. 2005). In the current study, we show that there are differences in the patterns of anatomical connectivity between the pregenual and subgenual portions of the human anterior cingulate gyrus. Although there is some overlap in connectivity patterns of the 2 subregions, with both connecting to midcingulate, FP, hypothalamus, and NAC, there are also important differences in strength of specific connections, and it is these differences that drive the connectivity-based parcellation. Note that the connectivity-based division between pACC and sACC does not require the tractography analysis to accurately identify all the connections of these 2 regions. The connectivity-based division depends only on detection of a change in connectivity between the 2 regions. This is a useful property as we know that diffusion tractography is potentially susceptible to false negatives and (less commonly) false positives, so that we cannot be sure that all connections with our ROIs have been identified. Note also that representations of

the pathways from pACC and sACC (Fig. 4), and the differences between them, are dependent on data quality, the performance of the tractography algorithm, and the thresholds used to display the paths. It is therefore not possible to make absolute conclusions about the absence of a given pathway. Nevertheless, there are apparent differences in the strength of connections from pACC and sACC to particular brain regions. The boundary that we defined based on anatomical connectivity was located slightly anterior but adjacent to the borders between area 25 and several more anterior areas, including 32, 24, and 10, that have been identified on the basis of cytoarchitectonics (Vogt et al. 1995; Ongur et al. 2003).

Like area 25 in the macaque (Porrino et al. 1981; Vogt and Pandya 1987; Van Hoesen et al. 1993; Kunishio and Haber 1994; Carmichael and Price 1995a, 1995b, 1996; Haber et al. 1995, 2006; Ongur et al. 1998; Rempel-Clower and Barbas 1998; Ferry et al. 2000; Freedman et al. 2000; Chiba et al. 2001), the sACC area in the present study was identified as having a high probability of connection with the NAC, hypothalamus, medial temporal lobe, the FP, and AMCC regions. Paths to the medial temporal lobe took 2 distinct routes: a direct path traveled laterally to the amygdala, whereas a second route traveled posteriorly along the fornix. This latter route is consistent with previously reported hippocampal inputs to medial prefrontal areas (Carmichael and Price 1995a, 1995b) and with reports that the hippocampal projections from adjacent orbitofrontal areas travel via the fornix (Cavada et al. 2000). This pathway could provide an anatomical substrate in the human brain for altered hippocampal-subgenual cingulate interactions that have been implicated by animal models of depression (Airan et al. 2007).

Our pACC region is likely to include parts of areas 32 and 24a and b. Like these regions in macaque, our human pACC region was shown to be strongly connected with the hypothalamus (Ongur et al. 1998; Rempel-Clower and Barbas 1998; Chiba et al. 2001) and midcingulate regions (Van Hoesen et al. 1993; Carmichael and Price 1995a, 1995b). The pregenual region in macaque is connected with the medial aspect of the OFC on the gyrus rectus (Morecraft et al. 1992; Carmichael and Price 1996; Cavada et al. 2000). Connections between pACC and medial OFC on the gyrus rectus were present in our human data albeit, as in the macaque (Carmichael and Price 1996), weaker than connections between sACC and medial OFC. The human pACC region was also found to have a high probability of connection with the FP and the same is true of areas 32 and 24 in the macaque (Carmichael and Price 1996). As in the macaque (Carmichael and Price 1996), connections between pACC and the frontopolar region, which included tissue on both medial and lateral surfaces, were stronger than those between sACC and the frontopolar region. Human pACC was found to have a connection with the fornix, albeit weaker than that found from sACC. In the macaque, area 32 is interconnected with the hippocampus (Carmichael and Price 1995a, 1995b) and although connections with the dorsomedial frontal cortex, including the dorsal ACC, are conveyed via the cingulum bundle, this is not true of more ventral regions on the medial surface (Morris et al. 1999); instead connections with more ventral frontal regions, such as the OFC, are known to be conveyed via the fornix in the macaque (Cavada et al. 2000).

A number of ACC regions are known to be interconnected with the amygdala (Van Hoesen et al. 1993; Morecraft et al. 2007). Although there was evidence for connections between

the amygdala and the pACC, their strength was weaker than that observed between sACC and amygdala. There is also evidence that areas 24a and b and area 32 connect with the amygdala in macaque (Carmichael and Price 1995a, 1995b). The strength of connections from different cingulate subregions is rarely systematically compared in macaque, but it has been claimed that, as we have found for the human brain, amygdala projections are stronger from the subgenual than the pregenual cingulate region in the monkey brain (Chiba et al. 2001).

Our evidence in the human brain is therefore largely consistent with available data from nonhuman primates and so confirms the relevance of work in macaques for understanding the functional anatomy of this region.

Although tracer studies have the advantage of providing unambiguous information about the presence or absence of an anatomical connection, our tractography results can complement conventional tracer studies by providing additional information on the route taken by particular connections; there has been a trend for recent tracer studies to provide little information about the routes taken by connections. Where these routes are known in the macaque, our results suggest the existence of similar pathways in the human brain (Cavada et al. 2000; Croxson et al. 2005; Schmahmann and Pandya 2006).

There are general methodological limitations to the use of diffusion tractography and connectivity-based parcellation that should be considered. Tractography cannot differentiate between anterograde and retrograde or direct and indirect connections. It is therefore critical that tractography findings are interpreted with reference to available data from gold standard tract-tracing studies in nonhuman primates, which provide unambiguous evidence on anatomical connectivity. Tractography is most sensitive to major fiber bundles, and small or tortuous paths are more challenging to track. Although use of a multi-fiber tractography algorithm will have increased our chances of tracking through regions of fiber complexity or crossing (Behrens et al. 2007), the approach is nevertheless potentially susceptible to false negatives. For example, in the current study, connection probability was found to be much higher between sACC and amygdala than between pACC and amygdala. Although, as mentioned, there is evidence for a similar difference in connection strengths in the macaque (Chiba et al. 2001), the difference appears to be particularly accentuated in the human diffusion tractography data. Whether the greater accentuation of the difference in the human data reflects a limitation of the diffusion tractography approach or a real difference in anatomy is unclear. Similarly, although animal studies have revealed differences between sACC and pACC connections to the shell and core of the NAC, respectively (Haber et al. 1995), the current resolution of imaging tractography limits delineations of these distinctions in the human brain.

There are also limitations of the connectivity-based parcellation approach used here. With this approach, connectivity measures are reduced to binary values (i.e., connected or not connected), for simplicity. Future studies should explore whether there is useful additional information in the continuous estimates of connection probability that are available. However, although the measures of connection probability provided by tractography can be used to make inferences about the relative strength of different fiber populations (as in Fig. 2), such conclusions must be made with care as other factors, such

as the length or geometry of a path, will also affect these measures (Johansen-Berg and Behrens 2006).

Electrode sites for patients who responded well to surgery were located within the sACC region, rather than the pACC region in this study, consistent with the intended surgical target. The effects of placing stimulating electrodes within the pACC region are not known. Although we found many similarities between the connection patterns of sACC and pACC, there were differences in connection strength to specific areas that might be important in mediating the therapeutic effects of DBS. For example, the sACC region was more strongly connected with the OFC, fornix, and medial temporal lobe in the vicinity of the amygdala and anterior hippocampus. Altered functional activity in some of these areas is present following chronic subgenual DBS (Mayberg et al. 2005). Furthermore, treatment response in depression can be predicted by the relative functional connectivity of subgenual cingulate (BA 25) to subcortical, hippocampal, and prefrontal regions (Seminowicz et al. 2004). These functional imaging results, together with the current tractography findings, suggest that relative balance among these connections, rather than absolute presence or absence of a connection, may be most critical in determining outcome. If impact on these specific subgenual-cortical, subcortical, and limbic paths is critical for mediating therapeutic effects of DBS, it is likely that stimulation of the pACC region would be less effective.

We reiterate that the primary motivation for this study was to evaluate regional variability of connectivity within the subgenual cingulate white matter to further understand potential mechanisms mediating clinical response to subgenual DBS in refractory depression (Mayberg et al. 2005). By expanding the ROI in this tractography analysis to include white matter in and around the intended surgical target, we demonstrated that the greatest anatomical variability was not within the subgenual region targeted at surgery but rather in the boundary between the sACC and pACC.

It is difficult to determine a general relationship between response to surgery and connectivity with small patient numbers and when projecting electrode contacts onto healthy control DWI data. The current study considered only patients with good outcome as the number of patients implanted and studied to date is relatively small, and therefore, an investigation of the relationship between electrode location and surgical outcome would be premature at this stage. Although approximately 60% of patients have a good clinical response (as defined by a greater than 50% reduction in the baseline Hamilton-17 Depression score), most others have a partial response. Preliminary indications suggest that there are no large differences in electrode location in space (in relation to the anterior-most and most ventral portion of the corpus callosum) between responders and nonresponders. However, given the known variation in sulcal anatomy of this region in the human brain (Paus, Otaky, et al. 1996; Paus, Tomaiuolo, et al. 1996; Yucel et al. 2001; Fornito et al. 2004, 2006), it is reasonable to expect that some interindividual variation in cytoarchitectonic boundaries exists. In addition, it is possible that anatomical variations in the origin of afferent and efferent pathways coursing through this region could account, at least in part, for the variable clinical response. An explicit analysis of the relationship between electrode location, anatomical connection patterns, clinical attributes, and surgical outcome within depressed patients will be needed to determine directly whether response to DBS

reflects differential impact on specific tracts or white matter variability among patients not currently seen in healthy controls. High-resolution DWI tractography studies of treatment-resistant depressed patients undergoing sACC white matter DBS are the focus of new studies to directly address this critical issue.

Nevertheless, this preliminary study identifies a number of common connections through the region consistently stimulated in a group of patients who all responded well to surgery and generates hypotheses that could be further tested in larger follow-up studies. Previous studies using diffusion imaging have demonstrated reduced fractional anisotropy in ACC and prefrontal white matter generally in depressed subjects (Taylor et al. 2004; Bae et al. 2006; Nobuhara et al. 2006); future studies using diffusion tractography should test the integrity of the specific tracts identified here in patients with mood disorders.

Critically, in the present study, the small sample and absence of a placebo-controlled design precludes any meaningful evaluation of the relationship between residual symptoms and electrode location variability in these patients. The connectivity patterns that we establish here suggest that future studies should compare electrode locations in patients with different response outcomes and test whether outcome depends on electrodes being located in regions that connect to specific structures including amygdala, hippocampus, NAC, midcingulate cortex, and OFC. This could be achieved through acquisition of preoperative diffusion data in individual patients in order to remove the potential confound of intersubject variability in local and connectional anatomy in the region. If a relationship between outcome and the connectivity patterns of targeted locations can be established, then acquisition of preoperative diffusion data could provide a useful tool for improved surgical targeting by allowing for individual delineation of the subgenual region with the effective connectivity fingerprint.

## Conclusion

This study has defined a reproducible distinction between connectivity patterns of the subgenual and pregenual cingulate within the ventral anterior cingulate region with important clinical implications for studies of major depression. These data in nondepressed healthy subjects suggest that the electrode target used in subgenual cingulate white matter DBS studies thus far is largely within the margins of a subgenual cingulate region defined by connections with OFC, AMCC, hypothalamus, NAC, hippocampus, and amygdala. These findings provide proof of principle support for the feasibility of characterizing these tracks in depressed patients and potentially for refining DBS electrode targeting using preoperatively acquired DWI data in individual patients. Such studies may further inform on mechanisms mediating response or nonresponse to other forms of antidepressant treatment.

## Funding

Wellcome Trust (to H.J.B.), UK Medical Research Council (to T.E.J.B.), Royal Society (to M.F.S.R.) and National Alliance for Research on Schizophrenia and Depression (to H.S.M.).

## Notes

We thank Matthew Robson for assistance with DTI data acquisition. *Conflict of Interest:* None declared.

Address correspondence to Dr Heidi Johansen-Berg, Oxford Centre for Functional MRI of the Brain, University of Oxford, John Radcliffe

Hospital, Headington, Oxford OX3 0HS, UK. Email: heidi@fmrib.ox.ac.uk.

## References

- Airan R, Meltzer L, Gong Y, Chen H, Deisseroth K. 2007. High-speed imaging reveals neurophysiological links to behavior in an animal model of depression. *Science*. 317:819–823.
- An X, Bandler R, Ongur D, Price JL. 1998. Prefrontal cortical projections to longitudinal columns in the midbrain periaqueductal gray in macaque monkeys. *J Comp Neurol*. 401:455–479.
- Anwander A, Tittgemeyer M, von Cramon DY, Friederici AD, Knosche TR. Connectivity-based parcellation of Broca's area. *Cereb Cortex*. 17:816–825.
- Bae JN, MacFall JR, Krishnan KR, Payne ME, Steffens DC, Taylor WD. 2006. Dorsolateral prefrontal cortex and anterior cingulate cortex white matter alterations in late-life depression. *Biol Psychiatry*. 60:1356–1363.
- Barbas H, Saha S, Rempel-Clover N, Ghashghaei T. 2003. Serial pathways from primate prefrontal cortex to autonomic areas may influence emotional expression. *BMC Neurosci*. 4:25–37.
- Barnard ST, Pothen A, Simon HD. 1995. A spectral algorithm for envelope reduction of sparse matrices. *Numer Lin Alg Appl*. 2:317–334.
- Beaulieu C, Allen PS. 1994. Determinants of anisotropic water diffusion in nerves. *Magn Reson Med*. 31:394–400.
- Behrens TE, Johansen-Berg H. 2005. Relating connectional architecture to grey matter function using diffusion imaging. *Philos Trans R Soc Lond B Biol Sci*. 360:903–911.
- Behrens TE, Johansen-Berg H, Jbabdi S, Rushworth MF, Woolrich MW. 2007. Probabilistic diffusion tractography with multiple fibre orientations: what can we gain? *Neuroimage*. 34:144–155.
- Behrens TE, Johansen-Berg H, Woolrich MW, Smith SM, Wheeler-Kingshott CA, Boulby PA, Barker GJ, Sillery EL, Sheehan K, Ciccarelli O, et al. 2003. Non-invasive mapping of connections between human thalamus and cortex using diffusion imaging. *Nat Neurosci*. 6:750–757.
- Behrens TEJ, Woolrich MW, Jenkinson M, Johansen-Berg H, Nunes RG, Clare S, Matthews PM, Brady JM, Smith SM. 2003. Characterization and propagation of uncertainty in diffusion-weighted MR imaging. *Magn Reson Med*. 50:1077–1088.
- Botteron KN, Raichle ME, Drevets WC, Heath AC, Todd RD. 2002. Volumetric reduction in left subgenual prefrontal cortex in early onset depression. *Biol Psychiatry*. 51:342–344.
- Carmichael ST, Price JL. 1994. Architectonic subdivision of the orbital and medial prefrontal cortex in the macaque monkey. *J Comp Neurol*. 346:366–402.
- Carmichael ST, Price JL. 1995a. Limbic connections of the orbital and medial prefrontal cortex in macaque monkeys. *J Comp Neurol*. 363:615–641.
- Carmichael ST, Price JL. 1995b. Sensory and premotor connections of the orbital and medial prefrontal cortex of macaque monkeys. *J Comp Neurol*. 363:642–664.
- Carmichael ST, Price JL. 1996. Connectional networks within the orbital and medial prefrontal cortex of macaque monkeys. *J Comp Neurol*. 371:179–207.
- Cavada C, Company T, Tejedor J, Cruz-Rizzolo RJ, Reinoso-Suarez F. 2000. The anatomical connections of the macaque monkey orbitofrontal cortex. A review. *Cereb Cortex*. 10:220–242.
- Chiba T, Kayahara T, Nakano K. 2001. Efferent projections of infralimbic and prelimbic areas of the medial prefrontal cortex in the Japanese monkey, *Macaca fuscata*. *Brain Res*. 888:83–101.
- Coryell W, Nopoulos P, Drevets W, Wilson T, Andreasen NC. 2005. Subgenual prefrontal cortex volumes in major depressive disorder and schizophrenia: diagnostic specificity and prognostic implications. *Am J Psychiatry*. 162:1706–1712.
- Croxson PL, Johansen-Berg H, Behrens TE, Robson MD, Pinski MA, Gross CG, Richter W, Richter MC, Kastner S, Rushworth MF. 2005. Quantitative investigation of connections of the prefrontal cortex in the human and macaque using probabilistic diffusion tractography. *J Neurosci*. 25:8854–8866.



- Drevets WC, Bogers W, Raichle ME. 2002. Functional anatomical correlates of antidepressant drug treatment assessed using PET measures of regional glucose metabolism. *Eur Neuropsychopharmacol.* 12:527-544.
- Evans AC, Collins DL, Mills SR, Brown ED, Kelly RL, Peters TM. 2003. 3D statistical neuroanatomical models from 305 MRI volumes. *Proc IEEE Nucl Sci Symp Med Imag Conf.* 95:1813-1817.
- Ferry AT, Ongur D, An X, Price JL. 2000. Prefrontal cortical projections to the striatum in macaque monkeys: evidence for an organization related to prefrontal networks. *J Comp Neurol.* 425:447-470.
- Fornito A, Whittle S, Wood SJ, Velakoulis D, Pantelis C, Yucel M. 2006. The influence of sulcal variability on morphometry of the human anterior cingulate and paracingulate cortex. *Neuroimage.* 33:843-854.
- Fornito A, Yucel M, Wood S, Stuart GW, Buchanan JA, Proffitt T, Anderson V, Velakoulis D, Pantelis C. 2004. Individual differences in anterior cingulate/paracingulate morphology are related to executive functions in healthy males. *Cereb Cortex.* 14:424-431.
- Freedman LJ, Insel TR, Smith Y. 2000. Subcortical projections of area 25 (subgenual cortex) of the macaque monkey. *J Comp Neurol.* 421:172-188.
- George MS, Ketter TA, Parekh PI, Horwitz B, Herscovitch P, Post RM. 1995. Brain activity during transient sadness and happiness in healthy women. *Am J Psychiatry.* 152:341-351.
- Goldapple K, Segal Z, Garson C, Lau M, Bieling P, Kennedy S, Mayberg H. 2004. Modulation of cortical-limbic pathways in major depression: treatment-specific effects of cognitive behavior therapy. *Arch Gen Psychiatry.* 61:34-41.
- Haber SN, Kim KS, Mailly P, Calzavara R. 2006. Reward-related cortical inputs define a large striatal region in primates that interface with associative cortical connections, providing a substrate for incentive-based learning. *J Neurosci.* 26:8368-8376.
- Haber SN, Kunishio K, Mizobuchi M, Lynd-Balta E. 1995. The orbital and medial prefrontal circuit through the primate basal ganglia. *J Neurosci.* 15:4851-4867.
- Hadjipavlou G, Duncleby P, Behrens TE, Tracey I. 2006. Determining anatomical connectivities between cortical and brainstem pain processing regions in humans: a diffusion tensor imaging study in healthy controls. *Pain.* 123:169-178.
- Heiervang E, Behrens TE, Mackay CE, Robson MD, Johansen-Berg H. 2006. Between session reproducibility and between subject variability of diffusion MR and tractography measures. *Neuroimage.* 33:867-877.
- Jenkinson M, Smith SM. 2001. Global optimisation for robust affine registration. *Med Image Anal.* 5:143-156.
- Johansen-Berg H, Behrens TE. 2006. Just pretty pictures? What diffusion tractography can add in clinical neuroscience. *Curr Opin Neurol.* 19:379-385.
- Johansen-Berg H, Behrens TE, Robson MD, Drobniak I, Rushworth MF, Brady JM, Smith SM, Higham DJ, Matthews PM. 2004. Changes in connectivity profiles define functionally distinct regions in human medial frontal cortex. *Proc Natl Acad Sci USA.* 101:13335-13340.
- Johansen-Berg H, Behrens TE, Sillery E, Ciccarelli O, Thompson AJ, Smith SM, Matthews PM. 2005. Functional-anatomical validation and individual variation of diffusion tractography-based segmentation of the human thalamus. *Cereb Cortex.* 15:31-39.
- Kennedy SH, Konarski JZ, Segal ZV, Lau MA, Bieling PJ, McIntyre RS, Mayberg HS. 2007. Differences in glucose metabolism between responders to cognitive behavioral therapy and venlafaxine in a 16-week randomized controlled trial. *Am J Psychiatry.* 164:778-788.
- Klein JC, Behrens TE, Robson MD, Mackay CE, Higham DJ, Johansen-Berg H. 2007. Connectivity-based parcellation of human cortex using diffusion MRI: establishing reproducibility, validity and observer independence in BA 44/45 and SMA/pre-SMA. *Neuroimage.* 34:204-211.
- Kunishio K, Haber SN. 1994. Primate cingulostriatal projection: limbic striatal versus sensorimotor striatal input. *J Comp Neurol.* 350:337-356.
- Liotti M, Mayberg HS, McGinnis S, Brannan SL, Jerabek P. 2002. Unmasking disease-specific cerebral blood flow abnormalities: mood challenge in patients with remitted unipolar depression. *Am J Psychiatry.* 159:1830-1840.
- Mayberg HS. 1997. Limbic-cortical dysregulation: a proposed model of depression. *J Neuropsychiatry Clin Neurosci.* 9:471-481.
- Mayberg HS. 2003. Modulating dysfunctional limbic-cortical circuits in depression: towards development of brain-based algorithms for diagnosis and optimised treatment. *Br Med Bull.* 65:193-207.
- Mayberg HS, Brannan SK, Tekell JL, Silva JA, Mahurin RK, McGinnis S, Jerabek PA. 2000. Regional metabolic effects of fluoxetine in major depression: serial changes and relationship to clinical response. *Biol Psychiatry.* 48:830-843.
- Mayberg HS, Liotti M, Brannan SK, McGinnis S, Mahurin RK, Jerabek PA, Silva JA, Tekell JL, Martin CC, Lancaster JL, et al. 1999. Reciprocal limbic-cortical function and negative mood: converging PET findings in depression and normal sadness. *Am J Psychiatry.* 156:675-682.
- Mayberg HS, Lozano AM, Voon V, McNeely HE, Seminowicz D, Hamani C, Schwalb JM, Kennedy SH. 2005. Deep brain stimulation for treatment-resistant depression. *Neuron.* 45:651-660.
- Morecraft RJ, Geula C, Mesulam MM. 1992. Cytoarchitecture and neural afferents of orbitofrontal cortex in the brain of the monkey. *J Comp Neurol.* 323:341.
- Morecraft RJ, McNeal DW, Stilwell-Morecraft KS, Gedney M, Ge J, Schroeder CM, van Hoesen GW. 2007. Amygdala interconnections with the cingulate motor cortex in the rhesus monkey. *J Comp Neurol.* 500:134-165.
- Morris R, Pandya DN, Petrides M. 1999. Fiber system linking the mid-dorsolateral frontal cortex with the retrosplenial/presubicular region in the rhesus monkey. *J Comp Neurol.* 407:183-192.
- Mottaghy FM, Keller CE, Gangitano M, Ly J, Thall M, Parker JA, Pascual-Leone A. 2002. Correlation of cerebral blood flow and treatment effects of repetitive transcranial magnetic stimulation in depressed patients. *Psychiatry Res.* 115:1-14.
- Nestler EJ, Barrot M, DiLeone RJ, Eisch AJ, Gold SJ, Monteggia LM. 2002. Neurobiology of depression. *Neuron.* 34:13-25.
- Nobler MS, Oquendo MA, Kegeles LS, Malone KM, Campbell CC, Sackeim HA, Mann JJ. 2001. Decreased regional brain metabolism after ect. *Am J Psychiatry.* 158:305-308.
- Nobuhara K, Okugawa G, Sugimoto T, Minami T, Tamagaki C, Takase K, Saito Y, Sawada S, Kinoshita T. 2006. Frontal white matter anisotropy and symptom severity of late-life depression: a magnetic resonance diffusion tensor imaging study. *J Neurol Neurosurg Psychiatry.* 77:120-122.
- Ongur D, An X, Price JL. 1998. Prefrontal cortical projections to the hypothalamus in macaque monkeys. *J Comp Neurol.* 401:480-505.
- Ongur D, Ferry AT, Price JL. 2003. Architectonic subdivision of the human orbital and medial prefrontal cortex. *J Comp Neurol.* 460:425-449.
- Paus T, Otaky N, Caramanos Z, MacDonald D, Zijdenbos A, D'Avirro D, Gutmans D, Holmes C, Tomaiuolo F, Evans AC. 1996. In vivo morphometry of the intrasulcal gray matter in the human cingulate, paracingulate, and superior-rostral sulci: hemispheric asymmetries, gender differences and probability maps. *J Comp Neurol.* 376:664-673.
- Paus T, Tomaiuolo F, Otaky N, MacDonald D, Petrides M, Atlas J, Morris R, Evans AC. 1996. Human cingulate and paracingulate sulci: pattern, variability, asymmetry, and probabilistic map. *Cereb Cortex.* 6:207.
- Pezawas L, Meyer-Lindenberg A, Drabant EM, Verchinski BA, Munoz KE, Kolachana BS, Egan MF, Mattay VS, Hariri AR, Weinberger DR. 2005. 5-HTTLPR polymorphism impacts human cingulate-amygdala interactions: a genetic susceptibility mechanism for depression. *Nat Neurosci.* 8:828-834.
- Porrino LJ, Crane AM, Goldman-Rakic PS. 1981. Direct and indirect pathways from the amygdala to the frontal lobe in rhesus monkeys. *J Comp Neurol.* 198:121-136.
- Ramnani N, Behrens TE, Johansen-Berg H, Richter MC, Pinski MA, Andersson JL, Rudebeck P, Ciccarelli O, Richter W, Thompson AJ, et al. 2005. The evolution of prefrontal inputs to the cortico-pontine system: diffusion imaging evidence from macaque monkeys and humans. *Cereb Cortex.* 16:811-818.

- Rempel-Clower NL, Barbas H. 1998. Topographic organization of connections between the hypothalamus and prefrontal cortex in the rhesus monkey. *J Comp Neurol*. 398:393–419.
- Rushworth MF, Behrens TE, Johansen-Berg H. 2006. Connection patterns distinguish 3 regions of human parietal cortex. *Cereb Cortex*. 16:1418–1430.
- Schmahmann JD, Pandya DN. 2006. *Fibre pathways of the brain*. New York: Oxford University Press.
- Seminowicz DA, Mayberg HS, McIntosh AR, Goldapple K, Kennedy S, Segal Z, Rafi-Tari S. 2004. Limbic-frontal circuitry in major depression: a path modeling metanalysis. *Neuroimage*. 22:409–418.
- Sillery E, Bittar RG, Robson MD, Behrens TE, Stein J, Aziz TZ, Johansen-Berg H. 2005. Connectivity of the human periventricular-periaqueductal gray region. *J Neurosurg*. 103:1030–1034.
- Smith SM. 2002. Fast robust automated brain extraction. *Hum Brain Mapp*. 17:143–155.
- Smith SM, Jenkinson M, Woolrich MW, Beckmann CF, Behrens TE, Johansen-Berg H, Bannister PR, De Luca M, Drobnjak I, Flitney DE, et al. 2004. Advances in functional and structural MR image analysis and implementation as FSL. *Neuroimage*. 23(Suppl 1):S208–S219.
- Stieltjes B, Kaufmann WE, van Zijl PC, Fredericksen K, Pearlson GD, Solaiyappan M, Mori S. 2001. Diffusion tensor imaging and axonal tracking in the human brainstem. *Neuroimage*. 14:723–735.
- Strakowski SM, Adler CM, Holland SK, Mills N, DelBello MP. 2004. A preliminary fMRI study of sustained attention in euthymic, unmedicated bipolar disorder. *Neuropsychopharmacology*. 29:1734–1740.
- Taylor WD, MacFall JR, Payne ME, McQuoid DR, Provenzale JM, Steffens DC, Krishnan KR. 2004. Late-life depression and microstructural abnormalities in dorsolateral prefrontal cortex white matter. *Am J Psychiatry*. 161:1293–1296.
- Van Hoesen GW, Morecraft RJ, Vogt BA. 1993. Connections of the monkey cingulate cortex. In: Vogt BA, Gabriel M, editors. *Neurobiology of cingulate cortex and limbic thalamus*. Boston: Birkhauser. p. 249–284.
- Vogt BA, Nimchinsky EA, Vogt LJ, Hof PR. 1995. Human cingulate cortex: surface features, flat maps, and cytoarchitecture. *J Comp Neurol*. 359:490–506.
- Vogt BA, Pandya DN. 1987. Cingulate cortex of the rhesus monkey: II. Cortical afferents. *J Comp Neurol*. 262:271–289.
- Vogt BA, Vogt L, Farber NB, Bush G. 2005. Architecture and neurocytology of monkey cingulate gyrus. *J Comp Neurol*. 485:218–239.
- Yucel M, Stuart G, Maruff P, Velakoulis D, Crowe S, Savage G, Pantelis C. 2001. Hemispheric and gender-related differences in the gross morphology of the anterior cingulate/paracingulate cortex in normal volunteers. An MRI morphometric study. *Cereb Cortex*. 11:17–25.